Title
The Transcription Factor NFAT Promotes Exhaustion of Activated CD8+ T Cells

Journal
Immunity, 42(2)

ISSN
1074-7613

Authors
Martinez, Gustavo J
Pereira, Renata M
Äijö, Tarmo
et al.

Publication Date
2015-02-01

DOI
10.1016/j.immuni.2015.01.006

Peer reviewed

HHS Public Access

Author manuscript

Immunity. Author manuscript; available in PMC 2016 February 17.

Published in final edited form as:

Immunity. 2015 February 17; 42(2): 265–278. doi:10.1016/j.immuni.2015.01.006.

The transcription factor NFAT promotes exhaustion of activated CD8+ T cells

Gustavo J. Martinez[1,11,*], **Renata M. Pereira**[1,*], **Tarmo Äijö**[1,2,*], **Edward Y. Kim**[3], **Francesco Marangoni**[3], **Matthew E. Pipkin**[1,4], **Susan Togher**[1], **Vigo Heissmeyer**[5,6], **Yi Chen Zhang**[7], **Shane Crotty**[8], **Edward D. Lamperti**[9], **K. Mark Ansel**[10], **Thorsten R. Mempel**[3], **Harri Lähdesmäki**[2], **Patrick G. Hogan**[1], and **Anjana Rao**[1]

[1]Department of Signaling and Gene Expression, La Jolla Institute for Allergy and Immunology, La Jolla, CA, 92037, USA [2]Department of Information and Computer Science, Aalto University School of Science, Aalto, FI-00076, Finland [3]Division of Rheumatology, Allergy, and Immunology, Center for Immunology and Inflammatory Diseases, Massachusetts General Hospital, Harvard Medical School, Boston, MA 02114, USA [4]Department of Cancer Biology, The Scripps Research Institute, Jupiter, FL, 33458, USA [5]Institute for Immunology, Helmholtz Zentrum München, Marchioninistrasse 25, 81377 Munich, Germany [6]Ludwig-Maximilians-Universität München, Institute for Immunology, Goethestrasse 31, 80336 Munich, Germany [7]Department of Radiology, St Lukes Roosevelt Hospital Center, New York, NY, 10019, USA [8]Department of Vaccine Discovery, La Jolla Institute for Allergy and Immunology, La Jolla, CA, 92037, USA [9]Immune Disease Institute, Harvard Medical School and Program in Cellular and Molecular Medicine, Children's Hospital Boston, Boston, MA 02115, USA [10]Department of Microbiology and Immunology, Sandler Asthma Basic Research Center, University of California, San Francisco, California 94143, USA

SUMMARY

Correspondence: Anjana Rao, Department of Signaling and Gene Expression, La Jolla Institute for Allergy and Immunology, 9420 Athena Circle, San Diego, CA, 92037, USA. arao@liai.org; Harri Lähdesmäki, Department of Information and Computer Science, Aalto University School of Science, Aalto, FI-00076, Finland. harri.lahdesmaki@aalto.fi.

[11]present address: The Scripps Research Institute, Jupiter, FL, 33458, USA

*These authors contributed equally to this work

AUTHOR CONTRIBUTIONS

G.J.M., R.M.P. and A.R. designed the experiments and analyzed data; G.J.M. and R.M.P. performed the experiments; T.A. and H.L. did the computational and statistical analysis of the data; A.R., G.J.M. and R.M.P. wrote the manuscript; E.Y.K., F.M. and T.R.M. designed and performed the tumor model and NFAT nuclear translocation (imaging) experiments; E.D.L. and K.M.A. constructed mice with floxed exon 3 of the gene encoding NFAT2; S.C. provided reagents; M.E.P., H.L. and P.G.H. provided input for experimental design and interpretation and critically evaluated the manuscript. V.H. and Y.C.Z. performed initial experiments relevant to the study.

The authors declare no conflict of interest.

During persistent antigen stimulation, $CD8^+$ T cells show a gradual decrease in effector function, referred to as exhaustion, which impairs responses in the setting of tumors and infections. Here we demonstrate that the transcription factor NFAT controls the program of T cell exhaustion. When expressed in cells, an engineered form of NFAT1 unable to interact with AP-1 transcription factors diminished T cell receptor (TCR) signaling, increased the expression of inhibitory cell surface receptors, and interfered with the ability of $CD8^+$ T cells to protect against *Listeria* infection and attenuate tumor growth *in vivo*. We defined the genomic regions occupied by endogenous and engineered NFAT1 in primary $CD8^+$ T cells, and showed that genes directly induced by the engineered NFAT1 overlapped with genes expressed in exhausted $CD8^+$ T cells in vivo. Our data show that NFAT promotes T cell anergy and exhaustion by binding at sites that do not require cooperation with AP-1.

INTRODUCTION

The transcription factor nuclear factor of activated T cells (NFAT) is well established as a key regulator of T cell activation (Crabtree and Olson, 2002; Hogan et al., 2003; Macian, 2005; Rao et al., 1997). Of the five members of the NFAT family, NFAT1-4 (also known as NFATc1-c4) are regulated by Ca^{2+}-calcineurin signaling; of these, NFAT1, NFAT2 and NFAT4 are expressed in cells of the immune system and have important roles in T cell development and function. All NFAT proteins make very similar contacts with DNA, but can have distinct expression patterns and functions as judged by the non-overlapping phenotypes of mice deficient in individual NFAT family members (Crabtree and Olson, 2002; Hogan et al., 2003; Macian, 2005). NFAT proteins interact with structurally unrelated Fos-Jun (AP-1) transcription factors to form cooperative NFAT: AP-1 complexes (Chen et al., 1998) that are critical for the induction of cytokine genes and other activation-associated genes (Macian et al., 2000). Adding to its versatility, NFAT forms dimers on palindromic κB-like sequence elements and can bind DNA as a monomer ((Chen et al., 1998; Giffin et al., 2003; Jin et al., 2010; Stroud et al., 2002); it also forms cooperative complexes with FOXP3, a transcription factor central to T regulatory function (Bandukwala et al., 2011; Chen et al., 1998; Macian et al., 2000; Wu et al., 2006). The ability to participate in multiple transcriptional complexes allows NFAT to contribute to different transcriptional programs depending on the cell type and signalling context in which it is activated (Hogan et al., 2003).

We previously linked NFAT not only to T cell activation, but also to T cell “tolerance” and “anergy” (Fehr et al., 2010; Heissmeyer et al., 2004; Macian et al., 2002), hyporesponsive states induced in T cells exposed to activating signals through the T cell receptor (TCR) in the absence of positive or presence of negative costimulatory signals (Nurieva et al., 2011). Another hyporesponsive state, termed $CD8^+$ T cell “exhaustion”, is induced in antigen-specific cytolytic T cells (CTLs) exposed to persistent antigen stimulation, for instance in the context of chronic viral infections and cancer (Schietinger and Greenberg, 2014; Wherry, 2011). Exhausted $CD8^+$ T cells display a transcriptional program distinct from that of functional effector or memory $CD8^+$ T cells (Wherry et al., 2007), characterized, for example, by the expression of several inhibitory cell surface receptors including PD-1, LAG3, TIM3, TIGIT and CTLA4 (Schietinger and Greenberg, 2014; Wherry, 2011).

However the key transcription factor(s) responsible for establishment of $CD8^+$ T cell exhaustion have not yet been identified (Wherry, 2011).

Here we show that NFAT elicits two parallel programs of $CD8^+$ T cell activation and exhaustion. To separate the NFAT-dependent programs of T cell activation and exhaustion, we generated an engineered version of NFAT1 that is incapable of AP-1 cooperation and therefore elicits no effector response. Expression of this engineered protein blunts T cell receptor (TCR) responses and elicits $CD8^+$ T cell exhaustion in mouse models of tumor growth and bacterial infection. The alternative NFAT-dependent transcriptional program is not limited to this simplified experimental situation, however, since NFAT-deficient $CD8^+$ T cells fail to express either effector cytokines or the inhibitory cell surface receptors PD-1, LAG3 and TIM3 that are characteristic of exhausted $CD8^+$ T cells. Using genome-wide analyses, we have defined the DNA elements functionally occupied by endogenous and engineered NFAT1 proteins, and have correlated occupancy with gene expression and *in vivo* function. Our results elucidate the transcriptional programs of hyporesponsiveness (anergy and exhaustion) in both $CD4^+$ and $CD8^+$ T cells, and show that NFAT proteins have a primary role.

RESULTS

We generated an engineered version of NFAT1, CA-RIT-NFAT1, that is constitutively nuclear and therefore constitutively active (CA) (Okamura et al., 2000) (Figure S1A), and also unable to interact with AP-1 ("RIT" refers to three residues – R468, I469 and T535 in mouse NFAT1 – that have been mutated to interfere selectively with the NFAT:AP-1 interaction (Macian et al., 2002; Macian et al., 2000)). The engineered CA-RIT-NFAT1 elicits no effector response, and so was a convenient tool for the genome-wide analysis. However, all three NFAT proteins present in T cells contribute to the negative regulatory program, as described below.

CA-RIT-NFAT1-expressing cells display defective TCR signaling

We used a bicistronic (IRES-GFP) retrovirus to introduce CA-RIT-NFAT1 into *in vitro*-activated $P14^+$ TCR transgenic T cells that also bore a deletion of the TCR Cα region (*Tcra*$^{-/-}$); the P14 TCR transgene recognizes a peptide from the gp33 protein of mouse lymphocytic choriomeningitis virus (LCMV) presented on H-$2D^b$. Naïve T cells were stimulated with anti-CD3 and anti-CD28, infected with IRES-GFP retrovirus expressing CA-RIT-NFAT1 or CA-RIT-NFAT1 with four point mutations in the DNA binding loop that abolish DNA binding (DBDmut-CA-RIT-NFAT1) (Jain et al., 1995) or empty vector (mock), and expanded with interleukin-2 (IL-2) to generate effector CTL (Pipkin et al., 2010). Expression of CA-RIT-NFAT1 in $CD8^+$ T cells substantially decreased IL-2 production in response to secondary stimulation (Figure S1B, S1C), even though CA-RIT-NFAT1 was expressed at amounts comparable to or lower than endogenous NFAT1 (Figure S1D, S1E).

To ask whether CA-RIT-NFAT1 expression impaired Ca^{2+} influx, we transduced $CD4^+$ T cells with CA-RIT-NFAT1 or empty vector (mock), labeled them with the Ca^{2+} indicators Fluo-4 or Fura-2, and quantified Ca^{2+} influx by flow cytometry (Figure S1F) or single-cell

imaging (Figure S1G). Compared to cells transduced with empty vector, cells expressing CA-RIT-NFAT1 displayed increased basal Ca^{2+} (Figure S1F) as well as reduced Ca^{2+} influx upon TCR stimulation (Figure S1F; Figure S1G, *left panel).* In contrast, Ca^{2+} influx was not diminished when TCR signaling was bypassed with thapsigargin treatment, which depletes endoplasmic reticulum (ER) Ca^{2+} stores by inhibiting the SERCA Ca^{2+}-ATPase (Figure S1G, *right panel).* Moreover, the increased phosphorylation of both ZAP-70 and PLCγ1 observed in control cells within minutes of re-stimulation with anti-CD3 and anti-CD28 was strongly impaired in cells expressing CA-RIT-NFAT1 (Figure S1H). Thus CA-RIT-NFAT1 expression affects two of the earliest steps of TCR signaling upstream of Ca^{2+} entry; other steps in the signaling window between TCR stimulation and ER store depletion could potentially also be impaired (Heissmeyer et al., 2004).

CA-RIT-NFAT1-expressing cells display impaired function in vivo

To test the biological effects of expressing CA-RIT-NFAT1 in $CD8^+$ T cells, we utilized an *in vivo Listeria* protection assay (modified from (Kaech et al., 2003)) (Figures 1A, S1I). Naïve $P14^+$ TCR transgenic $CD8^+$ T cells were stimulated with anti-CD3 and anti-CD28 and transduced one day later with CA-RIT-NFAT1, DBDmut-CA-RIT-NFAT1 or empty vector, then expanded with a low concentration of IL-2 *in vitro* to generate “memory-like” CD8 T cells (Pipkin et al., 2010). Transduced GFP^+ cells were then sorted by flow cytometry and transferred into naïve recipient mice; one day later, the mice were infected with genetically-modified *Listeria monocytogenes* expressing gp33 peptide (Figures 1A, S1I). Consistent with induction of an effective immune response against the *Listeria*-gp33, mice receiving mock-transduced gp33-specific T cells showed a significant reduction in bacterial colony-forming units (CFU) per spleen at 3 and 5 days after infection, compared to mice that did not receive any cells, whereas mice receiving cells transduced with CA-RIT-NFAT1 did not control *Listeria* infection effectively (Figures 1B, S1J). Thus CA-RIT-NFAT1 expression blunted the secondary immune response of CD8 T cells *in vivo*; some protection was still evident, however, indicating that T cell function was strongly diminished but not completely eliminated.

The adoptively transferred CA-RIT-NFAT1-expressing cells survived *in vivo* and were able to reach the infection site, although at lower percentages and total numbers compared to control cells, as judged by their presence in spleens of recipient mice 5 days after infection (Figure S1K and data not shown). Compared to cells transduced with DBDmut-CA-RIT-NFAT1, a higher percentage of CA-RIT-NFAT1-expressing cells expressed PD-1, TIM3 and LAG3, inhibitory surface receptors characteristic of exhausted T cells (Figure 1C–D).

To assess the impaired function of CA-RIT-NFAT1-expressing T cells in a different *in vivo* system, we utilized a tumor model in which influenza hemagglutinin (HA)-specific CL4 TCR transgenic T cells were transduced with CA-RIT-NFAT1 or DBDmut-CA-RIT-NFAT1 (Bauer et al., 2014; Marangoni et al., 2013). The cells were expanded *in vitro*, then transferred into congenic mice that had previously received HA-expressing CT26 tumors (CT26HA) subcutaneously in one flank and CT26 tumors that did not express HA in the contralateral flank. Tumor growth was assessed daily for 8 days after T cell transfer, and the expression of exhaustion-associated surface markers on the transferred cells was evaluated 3

days after transfer (Figure 1E). Control cells expressing the mutant DBDmut-CA-RIT-NFAT1 rejected the CT26HA antigen-expressing tumor without rejecting the contralateral tumor that did not express HA (Figure 1F), whereas cells expressing CA-RIT-NFAT1 showed diminished effector activity (Figure 1F) despite being present in the tumor at similar frequencies as cells expressing DBDmut-CA-RIT-NFAT1 (Figure 1G). As in the *Listeria* model, we observed a higher frequency of expression of the inhibitory markers PD-1, TIM3 and LAG3 in CA-RIT-NFAT1-expressing cells recovered from the tumor, compared to cells expressing DBDmut-CA-RIT-NFAT1 (Figure 1H–I).

Overall, even in the presence of endogenous NFAT proteins, CA-RIT-NFAT1 directly or indirectly upregulated the expression of several markers of T cell exhaustion on the $CD8^+$ T cells, and induced a negative feedback transcriptional program that attenuated $CD8^+$ T cell responses in two different settings *in vivo*.

Exhausted cells retain the ability to signal through NFAT

We asked whether NFAT could translocate to the nucleus in *in vivo* exhausted T cells. CT26HA tumors were implanted in $Thy1.1^+$ recipients that were then injected with regulatory T cells that recognize the HA antigen; this regimen induces exhaustion of endogenous $CD8^+$ T cells (Bauer et al., 2014). Ten days after tumor injection, mice were sacrificed, and tumor-infiltrating T cells were restimulated *ex vivo* with plate-bound anti-CD3s for 15 min. The cells were then fixed and sorted to separate the exhausted $PD\text{-}1^+TIM3^+$ cell and control PD-1TIM3- cell populations (Figure S2A), and stained for endogenous NFAT1 and DAPI (Figures 1J, S2B). The results show clearly that exhausted $CD8^+$ T cells are permissive for NFAT1 nuclear translocation upon activation through the TCR, although higher amounts of TCR stimulation are required than for non-exhausted cells (Figure 1K). Thus, *in vivo*-generated exhausted T cells can activate NFAT nuclear import, thus further reinforcing the exhaustion phenotype in the absence of AP-1 cooperation.

The transcriptional program induced by CA-RIT-NFAT1 overlaps with that of exhausted/anergic T cells

To define the transcriptional program induced by CA-RIT-NFAT1, we performed RNA-seq on $CD4^+$ and $CD8^+$ T cells transduced with empty or CA-RIT-NFAT1 retrovirus. Almost 2,000 genes showed altered expression ($p<0.05$) in CA-RIT-NFAT1-expressing $CD8^+$ T cells compared to mock-transduced cells, with approximately half of the genes showing increased expression and half decreased expression (Figure 2A, *top panel*). Similar results were obtained for $CD4^+$ T cells (Figure 2A, *bottom panel*). There was substantial overlap in genes differentially expressed in $CD4^+$ and $CD8^+$ T cells (one-tailed version of Fisher's exact test; p-value $<10^{-10}$), indicating that ectopic expression of CA-RIT-NFAT1 has similar transcriptional effects in both cell types (Figure 2B–D). There was also a highly significant overlap between the transcriptional profiles induced in $CD8^+$ and $CD4^+$ T cells by CA-RIT-NFAT1 and those observed in exhausted $CD8^+$ T cells and anergic $CD4^+$ T cells *in vivo* (22/56 genes and 99/371 genes respectively; p-value $<10^{-10}$) (Doering et al., 2012; Okamura et al., 2009; Wherry et al., 2007)(Figure 2E–F, Table 1, Figure S3E; Tables S1, S2).

CA-RIT-NFAT1-expressing T cells showed increased protein and mRNA expression of the inhibitory receptors LAG3, TIM3, PD-1 and GITR, based on flow cytometry, RNA-seq and quantitative PCR (Figure 2, S3A–D). Upregulation of the inhibitory receptors depended on NFAT1 DNA-binding, since it was not observed in cells expressing DBDmut-CA-RIT-NFAT1 (Figure S3B and data not shown), despite higher expression of this DNA-binding mutant compared to CA-RIT-NFAT1 (Figure S1E). Several genes coding for transcription factors (*Prdm1*, *Bhlhe40*, *Irf4*, *Ikzf2*, *Zeb2*, *Lass6*, *Tox*, *Eomes*) were recently identified in a network analysis (Doering et al., 2012) as potentially contributing to induction of the exhausted state; except for *Eomes*, all these transcription factors are also upregulated in CA-RIT-NFAT1-expressing cells (Figure S3E). Moreover, genes encoding other categories of negative regulatory proteins (e.g. diacylglycerol kinase, several phosphatases) were also expressed at higher amounts in cells expressing CA-RIT-NFAT1 compared to mock-transduced cells (Figure S3E). Thus even in the absence of interaction with AP-1, NFAT1 can induce exhaustion/anergy-associated genes in both $CD8^+$ and $CD4^+$ T cells.

CA-RIT-NFAT1 directly upregulates gene expression by binding to gene promoter regions

To determine which genes were likely to be direct targets of NFAT1 and CA-RIT-NFAT1, we analysed the genomic distribution of both proteins in $CD8^+$ T cells by chromatin immunoprecipitation followed by next-generation sequencing (ChIP-seq). Because only very small numbers of exhausted T cells can be obtained from mice, it was not possible to perform ChIP-seq experiments to define NFAT binding sites in exhausted $CD8^+$ T cells *in vivo*. Instead, we compared the genome-wide distribution of endogenous NFAT1 with that of ectopically expressed CA-RIT-NFAT1 in $CD8^+$ T cells left resting or stimulated *in vitro*.

Wild type (WT) or NFAT1-deficient naïve $P14^+$ $Tcra^{-/-}$ $CD8^+$ T cells were stimulated with anti-CD3 and anti-CD28, retrovirally transduced with empty vector or CA-RIT-NFAT1, and expanded in IL-2-containing media to yield effector CTL (Pipkin et al., 2010). 6 days later, cells were either left untreated (resting) or restimulated with PMA and ionomycin for 1 h, and chromatin was prepared and immunoprecipitated with anti-mouse NFAT1. Immunoprecipitation was specific, as evidenced by the low number of background peaks in NFAT1-deficient compared to control cells (Figure 3A). For subsequent analysis, we removed peaks also present in NFAT1-deficient cells and therefore considered background. As expected from the constitutive nuclear localization of CA-RIT-NFAT1 (Figure S1A), similar numbers of CA-RIT-NFAT1 peaks were observed in resting and restimulated NFAT1-deficient cells transduced with CA-RIT-NFAT1 (Figure 3B, *middle panels*). Comparison with the genome reference (mm9; Figure 3B, *right panel*) showed that both NFAT1 and CA-RIT-NFAT1 peaks were enriched at promoters/transcription start sites (TSS), exons and the first introns of genes (Figure 3B, 3C).

Genome browser views of genes encoding the inhibitory receptors PD-1, LAG3, TIM3, and Siglec-F illustrate that endogenous NFAT1 binds only after PMA and ionomycin stimulation (Figures 3D, S4A, *compare lines 1 and 2*), whereas CA-RIT-NFAT1 ChIP-seq peaks were observed in both resting and stimulated cells (*compare lines 5 and 6*). These ChIP-seq peaks were not observed in NFAT1-deficient T cells (*lines 3 and 4*), attesting to the specificity of our NFAT1 antibody. There was substantial overlap in ChIP-seq peaks for endogenous

NFAT1 and CA-RIT-NFAT1, as well as ChIP-seq peaks of CA-RIT-NFAT1 binding under resting and stimulated conditions (Figures 3D, S4A). Regions of NFAT1 but not CA-RIT-NFAT1 binding and vice versa are discussed below.

To understand the genome-wide binding patterns of NFAT1 and CA-RIT-NFAT1, we examined the ChIP-seq data in more detail. The distribution of CA-RIT-NFAT1-bound regions with respect to the nearest TSS differed depending on whether the genes transcribed from that TSS were up- or down-regulated by CA-RIT-NFAT1. The majority of upregulated genes had a CA-RIT-NFAT1 binding site within 2.5 kb of the TSS, but the binding sites were widely distributed with respect to the TSS of down-regulated genes (Figure 3E–F). These results suggest that CA-RIT-NFAT1 directly regulates the transcription of up-regulated genes by binding to sites in the vicinity of their promoter/TSS regions. Figure S4E shows the distribution of ChIP-seq peaks for other transcription factors with respect to the TSS (see Supplemental Discussion).

Sequence motif analyses of NFAT1 and CA-RIT-NFAT1 binding sites in CTLs

We used a motif-search algorithm (Homer) to compare sequence motifs enriched above background in NFAT1 and CA-RIT-NFAT1 ChIP-seq peaks (Figure 4). We considered ChIP-seq peaks that bound endogenous NFAT1 in stimulated cells (n ~29,000), and CA-RIT-NFAT1 under resting or stimulated conditions (n ~12,500 and ~14,500 respectively; Figure 4A). Notably, most NFAT1 ChIP-seq peaks did not overlap with CA-RIT-NFAT1 ChIP-seq peaks (Figure 4A, *left and middle panels*), suggesting that at these sites, NFAT binding is strongly stabilized by AP-1 (likely by ~20-fold or more; (Rao et al., 1997)). Among these is the well-known composite NFAT:AP-1 element in the *Il2* promoter (Chen et al., 1998; Jain et al., 1993; Jain et al., 1992) (Figure 4B, *left panel*). Similar composite elements are known to occur in the promoter and enhancer regions of several other calcium-responsive, cyclosporin A (CsA)-sensitive genes (Hogan et al., 2003; Rao et al., 1997).

In ChIP-seq peaks for endogenous NFAT1, the top two enriched motifs were the consensus monomer NFAT binding element (TTTCCA, complement TGGAAA) and a composite NFAT:AP-1 element (TGGAAAnnnTGA$^{G}/_{C}$TCA) (Figure 4C, *left panel*). Composite NFAT1:AP-1 element was the top enriched motif in the subset of NFAT1 ChIP-seq peaks that did not bind CA-RIT-NFAT1 (Figure 4D, *left panel*), whereas the monomer NFAT element was the top enriched motif in the subset of NFAT1 ChIP-seq peaks that also bound CA-RIT-NFAT1 (*data not shown*). As an example of the latter group, the proximal *Ctla4* promoter contains the monomer NFAT binding element TGGAAAAT (Figure 4B, *right panel*). These data confirm that the RIT mutation abolishes NFAT1:AP-1 interaction in cells as it does *in vitro*, and emphasize that despite its inability to engage in cooperative interactions with AP-1, CA-RIT-NFAT1 binds functionally and with measurable affinity to many NFAT1 binding sites.

Finally, a substantial number of the CA-RIT-NFAT1 ChIP-seq peaks detected in resting and stimulated cells were not observed in stimulated WT cells (Figure 4A, Table S4). These peaks showed low enrichment for NFAT:AP-1 composite sites (Figure 4C), and no enrichment for κB-like sites such as the site in the *Rnf128* promoter that binds NFAT1 homodimers [GTAACGTTTCC or GGATTCTTCC] (Soto-Nieves et al., 2009); *Rnf128*,

which encodes the E3 ligase Grail, is upregulated in anergic $CD4^+$ T cells (Fathman and Lineberry, 2007). Rather, the strong enrichment for consensus NFAT binding motifs in CA-RIT-NFAT1 ChIP-seq peaks suggests that monomer binding is dominant under these conditions, perhaps stabilized through protein-protein interactions with other partner proteins (see Supplementary Discussion).

NFAT-deficient $CD8^+$ T cells show diminished expression of exhaustion-associated inhibitory surface receptors

To examine the requirement for endogenous NFAT proteins in the regulation of exhaustion-associated genes, we bred our conventional gene-disrupted NFAT 1-deficient mice (Xanthoudakis et al., 1996) to mice deficient in NFAT2 in the T cell lineage (Figure S5A; see *Methods*). When differentiated into 'memory' CTL (Pipkin et al., 2010) and restimulated with PMA and ionomycin *in vitro*, NFAT1, 2-double deficient $CD8^+$ T cells showed clearly decreased induction of the effector cytokines IL-2 and IFN-γ compared to WT or singly NFAT1- or NFAT2-deficient $CD8^+$ T cells (Figure 5A); they also showed strongly diminished expression of the inhibitory surface receptors LAG3, TIM3 and PD-1 (Figure 5C and data not shown). The residual expression was due to NFAT4, the third NFAT protein present in immune cells: NFAT1, 2-deficient cells additionally transduced with shRNA against NFAT4 (Figure 5B) produced little or no IL-2 or interferon-γ (IFN-γ) upon restimulation (Figure 5A) and expressed little or no LAG3 and PD-1 either under resting conditions or after restimulation (Figure 5C), indicating that all 3 NFAT proteins contribute to $CD8^+$ T cell activation and exhaustion. Notably, there was no defect in proliferation of the NFAT1, 2-deficient $CD8^+$ T cells under these conditions (Figure S5B).

To ask whether NFAT family members were required for induction of the inhibitory receptors *in vivo*, we utilized a mouse model of infection with LCMV. WT, NFAT1-deficient, NFAT2-deficient or NFAT1 and NFAT2 double-deficient naïve $CD8^+$ $P14^+$ $Tcra^{-/-}$ T cells ($CD45.2^+$) were transferred into $CD45.1^+$ congenic mice. The mice were then infected with LCMV Armstrong 5 strain, which induces an acute infection (Wherry et al., 2007); eight days after infection, expression of the inhibitory receptors was determined in the transferred cells *ex vivo* (Figure 6A). Under these conditions *in vivo*, there was only a minor upregulation of LAG3; however, consistent with our *in vitro* studies, expression of all tested inhibitory receptors was strongly decreased in cells lacking both NFAT1 and NFAT2 (Figure 6A). Based on our *in vitro* experiments (Figure 5), the residual expression is most likely due to NFAT4.

We then evaluated the role of NFAT proteins using LCMV clone 13, which induces a chronic infection that leads to $CD8^+$ T cell exhaustion (Wherry et al., 2007). Mice lacking both NFAT1 and NFAT2 showed a dramatic decrease in the frequency of cells co-expressing PD-1 and TIM3 or LAG3 (Figure 6B). Together, our results support a direct role for NFAT family members in controlling the expression of inhibitory receptors in $CD8^+$ T cells, both in cell culture and in mice. Not all surface receptors are affected, however: for instance, the expression of CD44 was unimpaired in the absence of NFAT (*data not shown*).

DISCUSSION

In this study, we demonstrate that NFAT proteins, established regulators of T cell activation, also participate in the transcriptional program of $CD8^+$ T cell exhaustion. To dissect these two aspects of NFAT function, an essential tool was CA-RIT-NFAT1, an engineered form of NFAT1 that is both constitutively active and unable to interact with AP-1. Using this engineered protein, we have defined, for the first time, the genome-wide localization of NFAT1 under conditions where it does not cooperate with AP-1, as well as the NFAT-dependent transcriptional profile induced under these conditions. Moreover, we have used mice and T cells deficient for multiple NFAT family members to show that NFAT proteins directly and redundantly control cytokine expression as well as expression of exhaustion-related genes in $CD8^+$ T cells. We note that some of our detailed findings may be specific to the experimental systems used here, and may or may not apply to $CD8^+$ T cell exhaustion observed in other model systems or in human diseases.

Our data demonstrate that NFAT controls $CD8^+$ T cell exhaustion by binding directly to regulatory regions of many exhaustion-associated genes, including the *Pdcd1* (PD-1) and *Havcr2* (TIM3) promoters and *cis*-regulatory regions. Although NFAT1 and CA-RIT-NFAT1 occupy many overlapping sites, endogenous NFAT1 demonstrates a strong preference for canonical NFAT:AP-1 composite sites under stimulation conditions that also activate AP-1, whereas CA-RIT-NFAT1 shows a strong preference for monomeric NFAT sites. In some cases a two-step mechanism may apply: for instance, LAG3 is induced by Egr2 (Okamura et al., 2009), but NFAT1 binds near both the *Egr2* and *Lag3* TSSs (Figures 3D, S4A), suggesting that NFAT induces Egr2, after which NFAT and Egr2 cooperate to induce the expression of downstream target genes. Other pathways may also be involved: Notch (Mathieu et al., 2013) and type-I IFN (Terawaki et al., 2011) signaling regulate *Pdcd1* expression, and MEK kinase (Yoon et al., 2011) and T-bet (Anderson et al., 2010) regulate TIM3 expression.

The transcriptional program evoked by CA-RIT-NFAT1 in $CD8^+$ T cells overlaps with that observed in anergic $CD4^+$ T cells. mRNAs encoding E3 ligases (Fathman and Lineberry, 2007; Heissmeyer et al., 2004; Nurieva et al., 2011); phosphatases (Macian et al., 2002); and other signaling proteins including caspase 3, RGS proteins and diacylglycerol kinases (Joshi and Koretzky, 2013; Macian et al., 2002) are upregulated in both cases. The combined action of these negative regulators is likely to underlie the diminished activation of ZAP-70 and PLCγ1 and the consequent decrease in Ca^{2+} influx that we observe in CA-RIT-NFAT1-expressing T cells. We propose that this negative feedback program becomes dominant in $CD4^+$ T cells under conditions of ineffective costimulation (Mueller, 2010; Nurieva et al., 2011), and in $CD8^+$ T cells in the context of prolonged low-grade antigenic stimulation and/or inflammation, as encountered in chronic viral infections and cancer (Schietinger and Greenberg, 2014; Wherry, 2011).

Our data are consistent with previous studies on the role of NFAT in $CD8^+$ T cell exhaustion. Transcriptional profiling revealed higher expression of mRNA encoding NFAT2 in exhausted murine $CD8^+$ T cells isolated directly *ex vivo*, compared with all other T cell subsets (naïve, effector, memory) examined (Wherry et al., 2007); NFAT2 was shown to be

nuclear in tolerant $CD8^+$ T cells (Srinivasan and Frauwirth, 2007); and *Pdcd1* expression was shown to be regulated by NFAT2 (Oestreich et al., 2008). Although Agnellini et al. (2007) reported that NFAT2 was not present in the nucleus of exhausted $CD8^+$ T cells generated during chronic, high-dose LCMV infection in mice after 16 h of stimulation (they did not examine other NFAT proteins), an alternative interpretation of their data is that the short inducible isoform of NFAT2 (Chuvpilo et al., 2002) is poorly induced after restimulation of exhausted $CD8^+$ T cells. Indeed, the higher basal Ca^{2+} concentrations observed by Agnellini et al. in exhausted $CD8^+$ T cells and in CA-RIT-expressing cells in this report would increase NFAT-dependent induction of NFAT2 under basal conditions, as also observed in *ex vivo* exhausted cells (Wherry et al., 2007). Moreover, the blunted but not completely blocked Ca^{2+} influx in restimulated CA-RIT-NFAT1-expressing T cells is consistent with the observation that exhausted $CD8^+$ T cells support Ca^{2+} influx upon restimulation (Agnellini et al., 2007).

Although in these studies we engineered NFAT1 to eliminate NFAT:AP-1 cooperation, we propose that the NFAT-driven transcriptional program of feedback attenuation of T cell responses is a normal late feature of the immune response. Fos and Jun are elevated only transiently after stimulation (Jain et al., 1992), whereas NFAT can remain in the nucleus for long times even in response to very low elevations of intracellular Ca^{2+} (Dolmetsch et al., 1997; Marangoni et al., 2013; Oh-hora et al., 2008). Fos expression also declines during chronic infection despite antigen persistence, whereas NFAT2 expression is increased as discussed above (Wherry et al., 2007). Finally, exhausted $CD8^+$ T cells, defined in a tumor setting by PD-1 and TIM3 expression, can support the nuclear translocation of endogenous NFAT1 in response to high levels of TCR stimulation (Figure 1J). The combination of increased basal Ca^{2+} and a residual low concentration of Ca^{2+} signaling in anergized/exhausted cells would be sufficient for NFAT proteins to enter and remain in the nucleus to maintain the exhausted state. This would result in the transcriptional induction of exhaustion-related genes, whose expression requires NFAT but not NFAT:AP-1 cooperation as shown here.

Especially in the presence of antigen-specific T regulatory cells, tumor-infiltrating $CD8^+$ T cells display brief and unstable T cell-APC contacts which nevertheless are sufficient to induce prolonged NFAT-dependent transcription and establish a feedback mechanism that results in decreased T cell responses (Marangoni et al., 2013). Under these conditions, delayed export of NFAT from the nucleus results in a “memory” of previous signaling by NFAT (Marangoni et al., 2013). In contrast, signaling pathways regulating Ras, ERK and AP-1 activation exhibit a shorter signal memory (Faroudi et al., 2003), suggesting that tolerance/exhaustion programs are evoked in tumor-infiltrating T cells as a result of an altered balance between NFAT and other transcription factors including AP-1. Consistent with the likelihood that AP-1 does not participate in the exhaustion program, exhausted T cells show not only a higher expression of NFAT2 transcripts but also a concomitant reduction in the AP-1 family member Fos (Wherry, 2011). These findings complement our own observations that the strongest exhaustion phenotype is induced *in vitro* by CA-RIT-NFAT1, which cannot cooperate with AP-1.

The NFAT-dependent program of anergy/exhaustion has considerable relevance for the clinic. For instance, the PD-1-PD-1 ligand pathway is well established as a major inhibitory receptor pathway involved in T cell exhaustion (Barber et al., 2006), and blocking this pathway during chronic LCMV infection reinvigorates virus-specific $CD8^+$ T cell responses, resulting in lower viral loads (Barber et al., 2006). Moreover, antibodies to PD-1 and CTLA-4 have emerged as surprisingly effective agents for cancer immunotherapy (Schietinger and Greenberg, 2014), and individual or combined blockade of TIM3, PD-1 and LAG3 with antagonist antibodies has been shown to reverse exhaustion efficiently in $CD8^+$ T cells (Blackburn et al., 2009; Jin et al., 2010; Sakuishi et al., 2010). These therapies all act downstream of the NFAT-dependent program of anergy/exhaustion that we have described here.

Our data imply that rescuing AP-1 signaling in exhausted T cells would reverse the exhausted state, and so offer therapeutic value in chronic viral infections and cancer. Conversely, disrupting NFAT:AP-1 interaction would impose a hyporesponsive state, thus offering a potential therapeutic avenue for interfering with autoimmune responses that depend on NFAT:AP-1 cooperation. Since the RIT mutation does not interfere with NFAT:FOXP3 cooperation (data not shown), confirming predictions from the crystal structures that NFAT proteins make partially distinct contacts with Fos-Jun and FOXP proteins (Bandukwala et al., 2011; Chen et al., 1998; Wu et al., 2006), it might be possible to design reagents that disrupt the NFAT:AP-1 interaction but leave T regulatory function intact. Our future studies will address these possibilities.

EXPERIMENTAL PROCEDURES

Mice

$P14^+$ TCR transgenic ($P14^+$, Taconic) or OT-II mice were crossed with $Tcra^{-/-}$ mice (the P14 TCR transgene recognizes a peptide from the gp33 protein of mouse lymphocytic choriomeningitis virus (LCMV) presented on $H\text{-}2D^b$; the OT-II TCR transgene recognizes a peptide from ovalbumin presented on $I\text{-}A^b$). $P14^+Tcra^{-/-}$ mice were further crossed with NFAT1-deficient mice (Xanthoudakis et al., 1996) and with mice deficient in NFAT2 in the T cell lineage, obtained by breeding $CD4^{Cre}$ mice with mice in which exon 3 of the gene encoding NFAT2 was “floxed” (flanked with *LoxP* sites) (Figure S5A). The resulting mice lack both NFAT1 and NFAT2 in T cells (NFAT1, 2-deficient mice). CL4 mice express a transgenic TCR specific for $H\text{-}2K^d/HA_{515–523}$. All mice were maintained in specific pathogen-free barrier facilities and used according to protocols approved by the La Jolla Institute for Allergy and Immunology animal care and use committees.

Isolation, culture and Retroviral transduction of T Cells

Naïve $CD8^+$ or $CD4^+$ T cells were purified from spleen and lymph nodes harvested from 6- to 8-week-old mice by negative selection or by fluorescence-activated cell sorting. Cells were activated with anti-CD3 and anti-CD28 and maintained in the presence of IL-2. For cytokine production analyses, cells were restimulated with PMA and ionomycin. For retroviral transduction, viral supernatants were generated by transfection of PlatE cells.

GFP$^+$ or Ametrine$^+$ transduced cells were purified by fluorescence-activated cell sorting. *For more details, see* Supplemental Methods.

RNA-seq

For RNA-seq analysis, total RNA was used to isolate poly(A) RNA using the micropoly(A)purist kit (Ambion). The whole transcriptome library kit (Life Technologies) was used to prepare paired-end sequencing libraries. Sequencing was performed using a SOLID4 sequencer (Applied Biosystems) and the sequencing reads in color-space were mapped to the mm9 genome using Tophat (Trapnell et al., 2009). RNA-seq data is available under GEO accession number GSE64409. *For more details, see RNA-seq data analyses and Microarray data analysis in* Supplemental Methods.

ChIP-seq

Fixed Chromatin was sheared to yield 100–300 bp DNA fragments and immunoprecipitated with protein G/anti-NFAT1 antibody complexes. Immunoprecipitated and de-crosslinked DNA was end-repaired and ligated with barcoded SOLID adaptors. Ligated products were size selected by gel and PCR amplified. Barcoded libraries were sequenced in a SOLID4 sequencer (Applied Biosystems) and the reads were mapped using Bowtie (Langmead et al., 2009) to the mm9 genome in color-space. ChIP-seq data is available under GEO accession number GSE64409. *For more details, see ChIP-seq and motif analyses in* Supplemental Methods.

Lymphocytic choriomeningitis virus (LCMV) models

Six week-old WT mice or mice lacking NFAT1 and NFAT2 in T cells were infected i.v. with 3×10^6 PFU of LCMV clone 13. Eighteen days after infection, splenocytes were harvested and cells were stained with antibodies against CD8, CD44, PD-1, LAG3, TIM3 and tetramer (H2D^b-gp33-41). Expression of these markers was assessed by flow cytometry.

For adoptive transfer experiments, naïve P14$^+$*Tcra*$^{-/-}$ CD8$^+$ T cells were isolated from 6 week-old WT or NFAT1-deficient mice, or mice lacking NFAT2 or both NFAT1 and NFAT2 in T cells (all mice are CD45.2$^+$). 5×10^4 cells were adoptively transferred (i.v.) into B6.SJL (CD45.1$^+$) congenic mice, and then mice were infected with 2×10^5 PFU of LCMV Arm5 intraperitoneally. Eight days after infection, spleens were harvested, and cells stained for cell surface markers.

Listeria monocytogenes-gp33 *in vivo* protection assay

Naïve *P14*$^+$*Tcr*$^{-/-}$CD8$^+$T cells were activated with anti-CD3 and anti-CD28, transduced with CA-RIT-NFAT1, DBD-mut-CA-RIT-NFAT1 or empty vector (mock) and expanded with 10 U/ml IL-2 for 4 d. Then, GFP^{hi} cells were purified by FACS, and 5×10^4 cells were transferred into C56BL/6 recipient mice. One day later, mice were infected with 1×10^5 CFU Listeria-gp33, kindly provided by Dr. Rafi Ahmed (Kaech et al., 2003). On day 3–5, spleens were harvested and plated on brain heart infusion agar plates for colony counts and cells phenotypically characterized by FACS.

In vivo tumor model

Single-cell suspensions from spleens and LNs of CL4 mice were pulsed with 10 μM HA515–523 peptide for 1 hour at 37°C, then cultured with 10 ng/ml murine rIL-12 for the first 2 days and 20 ng/ml murine rIL-2 for the following 5 days as previously described (Bauer et al., 2014). Cells were then transferred to mice that had been inoculated s.c. in both shaved flanks with 10^6 viable CT26HA tumour cells suspended in 50 μl HBSS 7 days before. Tumor size was determined by caliper measurements of tumor length and width, and tumor volume was calculated as $(l \times w^2)/2$ (Bauer et al., 2014).

To induce exhausted T cells, CT26HA tumours were implanted in Thy1.1 recipients that were then injected with T regulatory cells that recognize the HA antigen (Bauer et al., 2014). Ten days after tumor injection, mice were sacrificed, and tumour-infiltrating T cells were restimulated *ex vivo* with plate-bound anti-CD3ε for 15 min, after which cells were fixed. Then, PD-1^+TIM3^+ and PD-1TIM3^- populations were sorted and stained for NFAT1 and DAPI, and then analyzed for confocal microscopy.

Supplementary Material

Refer to Web version on PubMed Central for supplementary material.

Acknowledgments

We thank Drs. Stephan Feske and Ariel Quintana for help with calcium influx experiments, Drs. Camille Fos and Sara Trifari for help with signaling experiments, Ryan Hastie for help in maintaining the colony, and Drs. Runqiang Chen and James Scott-Browne for providing retroviral constructs containing shCD4 and shNFAT4. We thank C. Kim, K. Gunst and L. Nosworthy at the La Jolla Institute Flow Cytometry Facility for help with cell sorting experiments, and Dr. G. Seumois and J. Day of the La Jolla Institute Sequencing facility, and the Genomics Core at The Scripps Research Institute in Florida, for help with next-generation sequencing. This work was funded by NIH grants R01 CA42471 (to AR), R01 AI40127 and AI84167 (to P.G.H. and A.R.), R01 AI095634 (to M.E.P.), EU FP7 grant EC-FP7-SYBILLA-201106 and the Academy of Finland Centre of Excellence in Molecular Systems Immunology and Physiology Research (to T.Ä. and H.L.) and German Research foundation SFB 1054 TP A03 to V.H. G.J.M. was supported by a postdoctoral fellowship from the Jane Coffin Childs Memorial Fund, R.M.P. by a postdoctoral fellowship from the Pew Latin American Fellows Program in the Biomedical Sciences, and T.Ä. by a graduate student fellowship from by the Finnish Doctoral Programme in Computational Sciences FICS.

References

Agnellini P, Wolint P, Rehr M, Cahenzli J, Karrer U, Oxenius A. Impaired NFAT nuclear translocation results in split exhaustion of virus-specific CD8+ T cell functions during chronic viral infection. Proc Natl Acad Sci U S A. 2007; 104:4565–4570. [PubMed: 17360564]

Anderson AC, Lord GM, Dardalhon V, Lee DH, Sabatos-Peyton CA, Glimcher LH, Kuchroo VK. T-bet, a Th1 transcription factor regulates the expression of Tim-3. Eur J Immunol. 2010; 40:859–866. [PubMed: 20049876]

Bandukwala HS, Wu Y, Feuerer M, Chen Y, Barboza B, Ghosh S, Stroud JC, Benoist C, Mathis D, Rao A, Chen L. Structure of a domain-swapped FOXP3 dimer on DNA and its function in regulatory T cells. Immunity. 2011; 34:479–491. [PubMed: 21458306]

Barber DL, Wherry EJ, Masopust D, Zhu B, Allison JP, Sharpe AH, Freeman GJ, Ahmed R. Restoring function in exhausted CD8 T cells during chronic viral infection. Nature. 2006; 439:682–687. [PubMed: 16382236]

Bauer CA, Kim EY, Marangoni F, Carrizosa E, Claudio NM, Mempel TR. Dynamic Treg interactions with intratumoral APCs promote local CTL dysfunction. J Clin Invest. 2014; 124:2425–2440. [PubMed: 24812664]

Blackburn SD, Shin H, Haining WN, Zou T, Workman CJ, Polley A, Betts MR, Freeman GJ, Vignali DA, Wherry EJ. Coregulation of CD8+ T cell exhaustion by multiple inhibitory receptors during chronic viral infection. Nat Immunol. 2009; 10:29–37. [PubMed: 19043418]

Chen L, Glover JN, Hogan PG, Rao A, Harrison SC. Structure of the DNA-binding domains from NFAT, Fos and Jun bound specifically to DNA. Nature. 1998; 392:42–48. [PubMed: 9510247]

Chuvpilo S, Jankevics E, Tyrsin D, Akimzhanov A, Moroz D, Jha MK, Schulze-Luehrmann J, Santner-Nanan B, Feoktistova E, Konig T, et al. Autoregulation of NFATc1/A expression facilitates effector T cells to escape from rapid apoptosis. Immunity. 2002; 16:881–895. [PubMed: 12121669]

Crabtree GR, Olson EN. NFAT signaling: choreographing the social lives of cells. Cell. 2002; 109(Suppl):S67–79. [PubMed: 11983154]

Doering TA, Crawford A, Angelosanto JM, Paley MA, Ziegler CG, Wherry EJ. Network analysis reveals centrally connected genes and pathways involved in CD8+ T cell exhaustion versus memory. Immunity. 2012; 37:1130–1144. [PubMed: 23159438]

Dolmetsch RE, Lewis RS, Goodnow CC, Healy JI. Differential activation of transcription factors induced by Ca2+ response amplitude and duration. Nature. 1997; 386:855–858. [PubMed: 9126747]

Faroudi M, Zaru R, Paulet P, Muller S, Valitutti S. Cutting edge: T lymphocyte activation by repeated immunological synapse formation and intermittent signaling. J Immunol. 2003; 171:1128–1132. [PubMed: 12874197]

Fathman CG, Lineberry NB. Molecular mechanisms of CD4+ T-cell anergy. Nat Rev Immunol. 2007; 7:599–609. [PubMed: 17612584]

Fehr T, Lucas CL, Kurtz J, Onoe T, Zhao G, Hogan T, Vallot C, Rao A, Sykes M. A CD8 T cell-intrinsic role for the calcineurin-NFAT pathway for tolerance induction in vivo. Blood. 2010; 115:1280–1287. [PubMed: 20007805]

Giffin MJ, Stroud JC, Bates DL, von Koenig KD, Hardin J, Chen L. Structure of NFAT1 bound as a dimer to the HIV-1 LTR kappa B element. Nat Struct Biol. 2003; 10:800–806. [PubMed: 12949493]

Heissmeyer V, Macian F, Im SH, Varma R, Feske S, Venuprasad K, Gu H, Liu YC, Dustin ML, Rao A. Calcineurin imposes T cell unresponsiveness through targeted proteolysis of signaling proteins. Nat Immunol. 2004; 5:255–265. [PubMed: 14973438]

Hogan PG, Chen L, Nardone J, Rao A. Transcriptional regulation by calcium, calcineurin, and NFAT. Genes Dev. 2003; 17:2205–2232. [PubMed: 12975316]

Jain J, Burgeon E, Badalian TM, Hogan PG, Rao A. A similar DNA-binding motif in NFAT family proteins and the Rel homology region. J Biol Chem. 1995; 270:4138–4145. [PubMed: 7876165]

Jain J, McCaffrey PG, Miner Z, Kerppola TK, Lambert JN, Verdine GL, Curran T, Rao A. The T-cell transcription factor NFATp is a substrate for calcineurin and interacts with Fos and Jun. Nature. 1993; 365:352–355. [PubMed: 8397339]

Jain J, Valge-Archer VE, Rao A. Analysis of the AP-1 sites in the IL-2 promoter. J Immunol. 1992; 148:1240–1250. [PubMed: 1737937]

Jin HT, Anderson AC, Tan WG, West EE, Ha SJ, Araki K, Freeman GJ, Kuchroo VK, Ahmed R. Cooperation of Tim-3 and PD-1 in CD8 T-cell exhaustion during chronic viral infection. Proc Natl Acad Sci U S A. 2010; 107:14733–14738. [PubMed: 20679213]

Joshi RP, Koretzky GA. Diacylglycerol kinases: regulated controllers of T cell activation, function, and development. Int J Mol Sci. 2013; 14:6649–6673. [PubMed: 23531532]

Kaech SM, Tan JT, Wherry EJ, Konieczny BT, Surh CD, Ahmed R. Selective expression of the interleukin 7 receptor identifies effector CD8 T cells that give rise to long-lived memory cells. Nat Immunol. 2003; 4:1191–1198. [PubMed: 14625547]

Langmead B, Trapnell C, Pop M, Salzberg SL. Ultrafast and memory-efficient alignment of short DNA sequences to the human genome. Genome Biol. 2009; 10:R25. [PubMed: 19261174]

Macian F. NFAT proteins: key regulators of T-cell development and function. Nat Rev Immunol. 2005; 5:472–484. [PubMed: 15928679]

Macian F, Garcia-Cozar F, Im SH, Horton HF, Byrne MC, Rao A. Transcriptional mechanisms underlying lymphocyte tolerance. Cell. 2002; 109:719–731. [PubMed: 12086671]

Macian F, Garcia-Rodriguez C, Rao A. Gene expression elicited by NFAT in the presence or absence of cooperative recruitment of Fos and Jun. Embo J. 2000; 19:4783–4795. [PubMed: 10970869]

Marangoni F, Murooka TT, Manzo T, Kim EY, Carrizosa E, Elpek NM, Mempel TR. The transcription factor NFAT exhibits signal memory during serial T cell interactions with antigen-presenting cells. Immunity. 2013; 38:237–249. [PubMed: 23313588]

Mathieu M, Cotta-Grand N, Daudelin JF, Thebault P, Labrecque N. Notch signaling regulates PD-1 expression during CD8(+) T-cell activation. Immunol Cell Biol. 2013; 91:82–88. [PubMed: 23070399]

Mueller DL. Mechanisms maintaining peripheral tolerance. Nat Immunol. 2010; 11:21–27. [PubMed: 20016506]

Nurieva RI, Liu X, Dong C. Molecular mechanisms of T-cell tolerance. Immunol Rev. 2011; 241:133–144. [PubMed: 21488895]

Oestreich KJ, Yoon H, Ahmed R, Boss JM. NFATc1 regulates PD-1 expression upon T cell activation. J Immunol. 2008; 181:4832–4839. [PubMed: 18802087]

Oh-hora M, Yamashita M, Hogan PG, Sharma S, Lamperti E, Chung W, Prakriya M, Feske S, Rao A. Dual functions for the endoplasmic reticulum calcium sensors STIM1 and STIM2 in T cell activation and tolerance. Nat Immunol. 2008; 9:432–443. [PubMed: 18327260]

Okamura H, Aramburu J, Garcia-Rodriguez C, Viola JP, Raghavan A, Tahiliani M, Zhang X, Qin J, Hogan PG, Rao A. Concerted dephosphorylation of the transcription factor NFAT1 induces a conformational switch that regulates transcriptional activity. Mol Cell. 2000; 6:539–550. [PubMed: 11030334]

Okamura T, Fujio K, Shibuya M, Sumitomo S, Shoda H, Sakaguchi S, Yamamoto K. CD4+CD25-LAG3+ regulatory T cells controlled by the transcription factor Egr-2. Proc Natl Acad Sci U S A. 2009; 106:13974–13979. [PubMed: 19666526]

Pipkin ME, Sacks JA, Cruz-Guilloty F, Lichtenheld MG, Bevan MJ, Rao A. Interleukin-2 and inflammation induce distinct transcriptional programs that promote the differentiation of effector cytolytic T cells. Immunity. 2010; 32:79–90. [PubMed: 20096607]

Rao A, Luo C, Hogan PG. Transcription factors of the NFAT family: regulation and function. Annu Rev Immunol. 1997; 15:707–747. [PubMed: 9143705]

Sakuishi K, Apetoh L, Sullivan JM, Blazar BR, Kuchroo VK, Anderson AC. Targeting Tim-3 and PD-1 pathways to reverse T cell exhaustion and restore anti-tumor immunity. J Exp Med. 2010; 207:2187–2194. [PubMed: 20819927]

Schietinger A, Greenberg PD. Tolerance and exhaustion: defining mechanisms of T cell dysfunction. Trends in immunology. 2014; 35:51–60. [PubMed: 24210163]

Soto-Nieves N, Puga I, Abe BT, Bandyopadhyay S, Baine I, Rao A, Macian F. Transcriptional complexes formed by NFAT dimers regulate the induction of T cell tolerance. J Exp Med. 2009; 206:867–876. [PubMed: 19307325]

Srinivasan M, Frauwirth KA. Reciprocal NFAT1 and NFAT2 nuclear localization in CD8+ anergic T cells is regulated by suboptimal calcium signaling. J Immunol. 2007; 179:3734–3741. [PubMed: 17785810]

Stroud JC, Lopez-Rodriguez C, Rao A, Chen L. Structure of a TonEBP-DNA complex reveals DNA encircled by a transcription factor. Nat Struct Biol. 2002; 9:90–94. [PubMed: 11780147]

Terawaki S, Chikuma S, Shibayama S, Hayashi T, Yoshida T, Okazaki T, Honjo T. IFN-alpha directly promotes programmed cell death-1 transcription and limits the duration of T cell-mediated immunity. J Immunol. 2011; 186:2772–2779. [PubMed: 21263073]

Trapnell C, Pachter L, Salzberg SL. TopHat: discovering splice junctions with RNA-Seq. Bioinformatics. 2009; 25:1105–1111. [PubMed: 19289445]

Wherry EJ. T cell exhaustion. Nat Immunol. 2011; 12:492–499. [PubMed: 21739672]

Wherry EJ, Ha SJ, Kaech SM, Haining WN, Sarkar S, Kalia V, Subramaniam S, Blattman JN, Barber DL, Ahmed R. Molecular signature of CD8+ T cell exhaustion during chronic viral infection. Immunity. 2007; 27:670–684. [PubMed: 17950003]

Wu Y, Borde M, Heissmeyer V, Feuerer M, Lapan AD, Stroud JC, Bates DL, Guo L, Han A, Ziegler SF, et al. FOXP3 controls regulatory T cell function through cooperation with NFAT. Cell. 2006; 126:375–387. [PubMed: 16873067]

Xanthoudakis S, Viola JP, Shaw KT, Luo C, Wallace JD, Bozza PT, Luk DC, Curran T, Rao A. An enhanced immune response in mice lacking the transcription factor NFAT1. Science. 1996; 272:892–895. [PubMed: 8629027]

Yoon SJ, Lee MJ, Shin DC, Kim JS, Chwae YJ, Kwon MH, Kim K, Park S. Activation of mitogen activated protein kinase-Erk kinase (MEK) increases T cell immunoglobulin mucin domain-3 (TIM-3) transcription in human T lymphocytes and a human mast cell line. Mol Immunol. 2011; 48:1778–1783. [PubMed: 21621846]

HIGHLIGHTS

- NFAT proteins induce a transcriptional program of $CD8^+$ T cell exhaustion
- $CD8^+$ T cells lacking NFAT fail to express inhibitory surface receptors
- An engineered NFAT that cannot cooperate with AP-1 strongly induces exhaustion
- The engineered NFAT1 blunts TCR signaling and impairs $CD8^+$ function *in vivo*

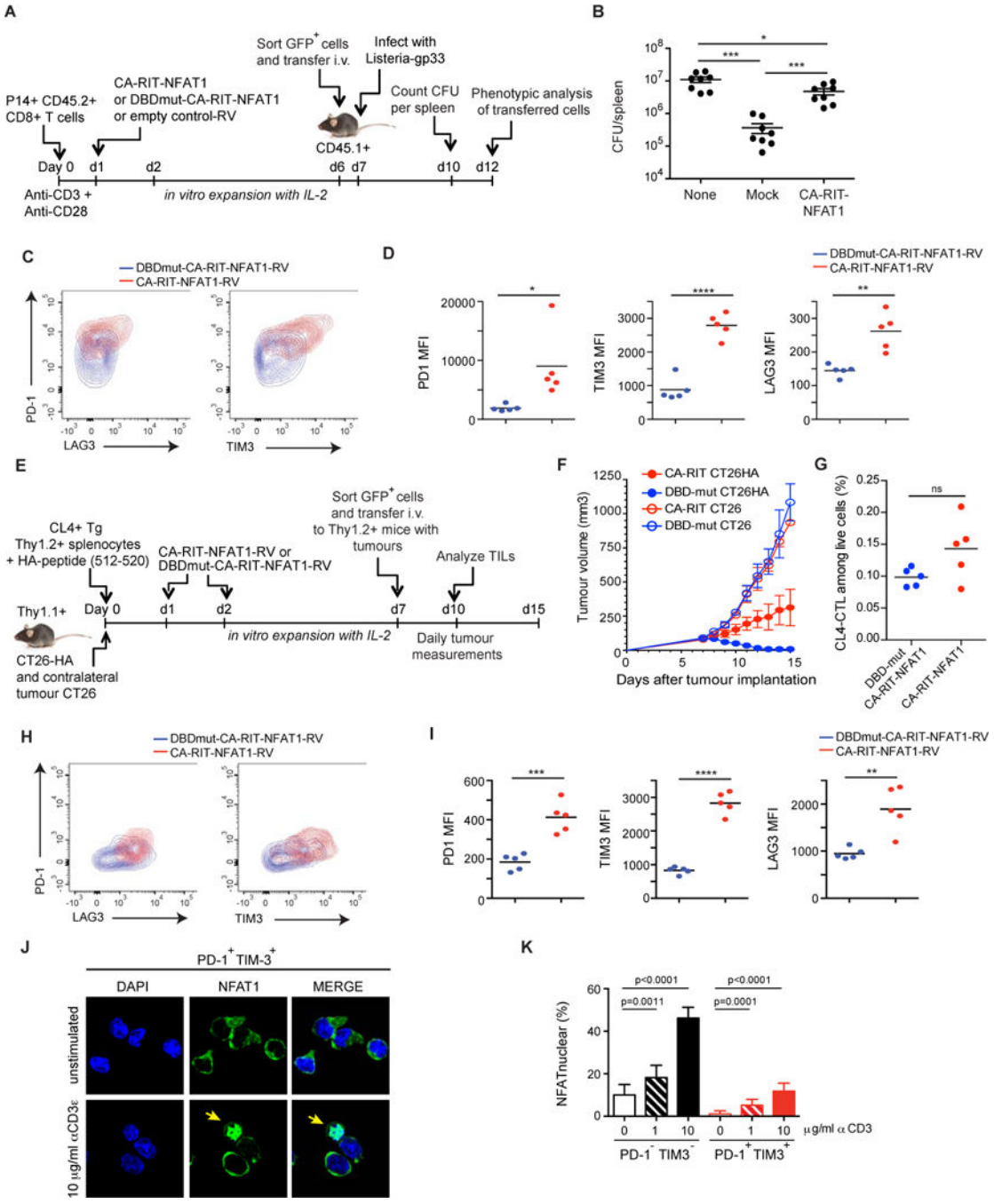

Figure 1. CTLs expressing a constitutively active NFAT1 incapable of cooperating with AP-1 have impaired *in vivo* function

(A–D) GFP^{hi} P14^{+} CD8^{+} T cells expressing CA-RIT-NFAT1 or its DNA-binding mutant were transferred to CD45.1^{+} congenic mice, which were infected one day later with gp33-expressing *Listeria monocytogenes.* (**B**) Three days after infection, total bacterial colony-forming units (CFU) per spleen were determined (each dot represents a mouse; mean ± SEM. *, $p < 0.05$; ***, $p < 0.001$ using t test). A representative experiment of two is shown. (**C**) Five days after infection, co-expression of PD-1 and LAG3 or PD-1 and TIM3 on

transferred cells ($CD45.2^+$) was determined by flow cytometry. Representative contour plots are shown. (**D**) The mean fluorescence intensity (MFI) for each receptor is shown. p values were calculated using t-test. *, $p < 0.05$; **, $p < 0.005$; ****, $p< 0.0001$. (**E-I**) GFP^{hi} $Thy1.2^+$ $CL4^+$ TCR transgenic $CD8^+$ T cells expressing CA-RIT-NFAT1 or its DNA-binding mutant were transferred to $Thy1.1^+$ congenic mice, injected seven 7 days previously with CT26 and CT26HA tumor cells in contralateral flanks. (**F**) Tumor growth was determined on a daily basis after cell transfer. (**G–I**) Characterization of transferred cells 3 days after transfer. (**G**) Frequency of tumor-infiltrating CA-RIT-NFAT1- and DBDmut-CA-RIT-NFAT1-transduced cells in live gate. (**H–I**) Co-expression of inhibitory receptors on transferred cells determined by flow cytometry. Representative contour plots are shown. (**I**) MFI for each receptor is shown. p values were calculated using t-test. **, $p < 0.005$; ***, $p < 0.0005$; ****, $p< 0.0001$. (**J–K**) NFAT nuclear translocation in exhausted cells. Single cell suspensions from 10 day-old CT26HA tumors were stimulated *ex vivo* with increasing doses of plate-bound anti-CD3 and immediately fixed. (**J)** Confocal images of *ex vivo*-stimulated exhausted cells ($CD45^+CD8^+PD\text{-}1^+Tim\text{-}3^+$) purified by cell sorting and stained for endogenous NFAT1. Arrows highlight cells with nuclear NFAT1. Scale bar 10 μm. (**K)** NFAT nuclear translocation in exhausted ($PD\text{-}1^+TIM3^+$) and non-exhausted ($PD\text{-}1^-TIM3^-$) $CD8^+$ tumor-infiltrating lymphocytes calculated from confocal images in **J**. Means ± S.D. of >10 fields of view (at least 720 cells) are shown. p values were calculated by t-test. See also Figures S1, S2.

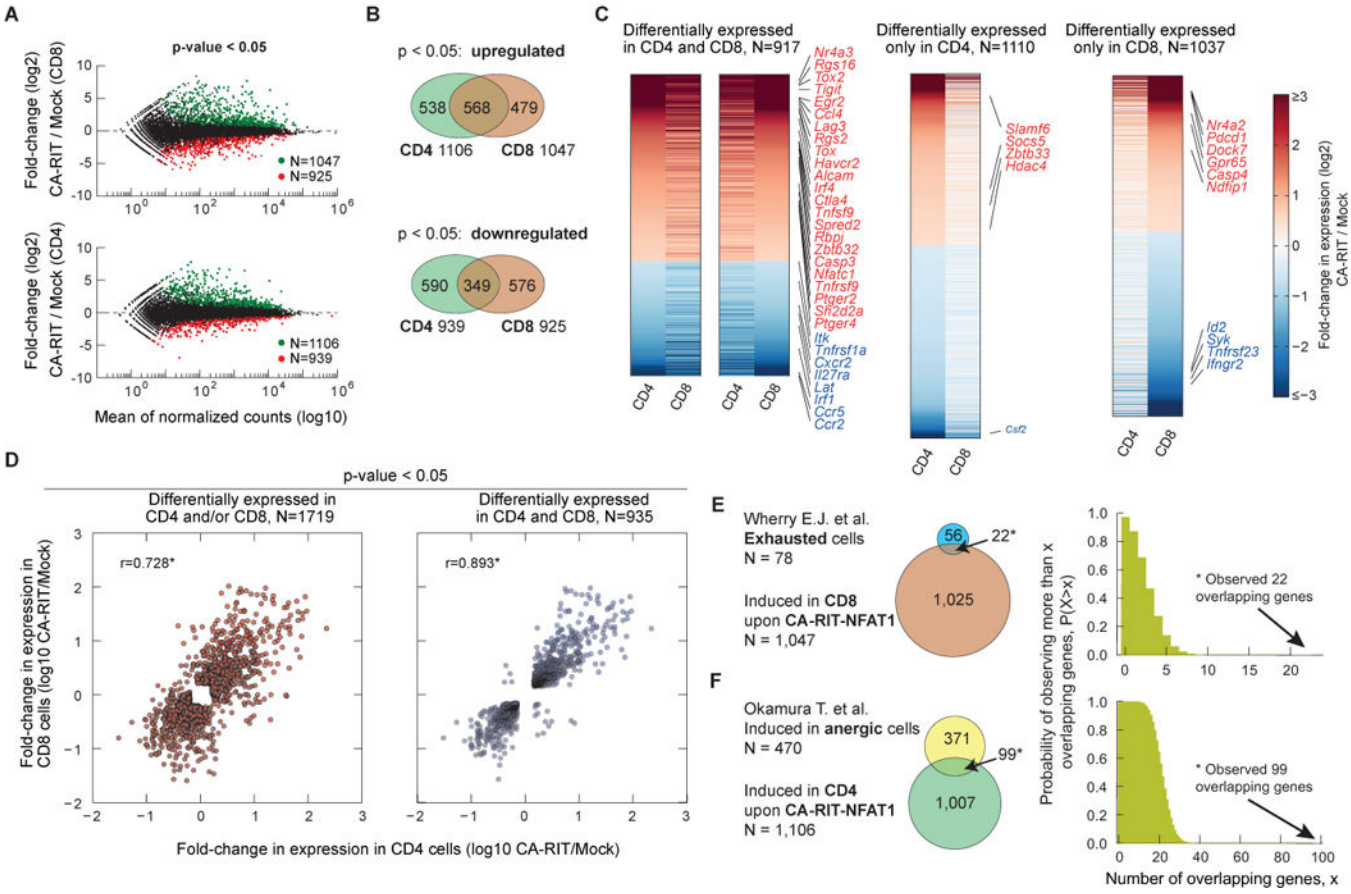

Figure 2. The transcriptional program induced by CA-RIT-NFAT1 in T cells overlaps with that of *in vivo* exhausted/anergic T cells

(**A**) Genes whose expression is altered upon CA-RIT-NFAT1 expression in $CD8^+$ (*top panel*) or $CD4^+$ (*bottom panel*) T cells. Changes in gene expression in CA-RIT-NFAT1-expressing *versus* mock-transduced cells plotted against overall gene expression. (**B**) Venn diagram displaying numbers of genes significantly induced (*top panel*) or downregulated (*bottom panel*) in $CD8^+$ and/or $CD4^+$ T cells. (**C**) Heatmap representation of changes in gene expression in CA-RIT-NFAT1-transduced over mock-transduced $CD4^+$ and $CD8^+$ T cells ($p<0.05$). Each horizontal line represents one gene, ordered by gene expression (highest to lowest fold change). 18 genes which showed opposite trends in $CD4^+$ and $CD8^+$ T cells were omitted (*depicted in the upper left and lower right quadrants of* **D**, *right panel*). (**D**) Scatter plot representing changes in gene expression in CA-RIT-NFAT1-transduced cells versus mock-transduced cells (RPKM values from RNA-Seq) in $CD8^+$ T cells (y axis) versus $CD4^+$ T cells (x-axis). Each dot represents a gene. Pearson correlation coefficients are indicated. *, $p<10^{-10}$. (**E**) Overlap of genes significantly upregulated upon CA-RIT-NFAT1 expression in $CD8^+$ T cells with genes significantly upregulated in either *in vivo*-generated exhausted $CD8^+$ T cells (*top*) (cluster #1,(Wherry et al., 2007)), or in anergic $CD4^+$ $CD25^-$ $CD45RB^{lo}$ $LAG3^+$ anergic T cells compared to $CD4^+$ $CD25^-$ $CD45RB^{lo}$ $Lag3^-$ T cells (*bottom*) (Okamura et al., 2009). (**F**) Plots show the probability of observing more than N overlapping genes if sets with 1,047 and 78 genes (*top*) or 1,007 and 480 genes

(*bottom*) are sampled randomly from the set of all genes. * p-value for the overlap < 10^{-10} (one-tailed Fisher's exact test). See also Tables S1, S2, S6 and Figure S3.

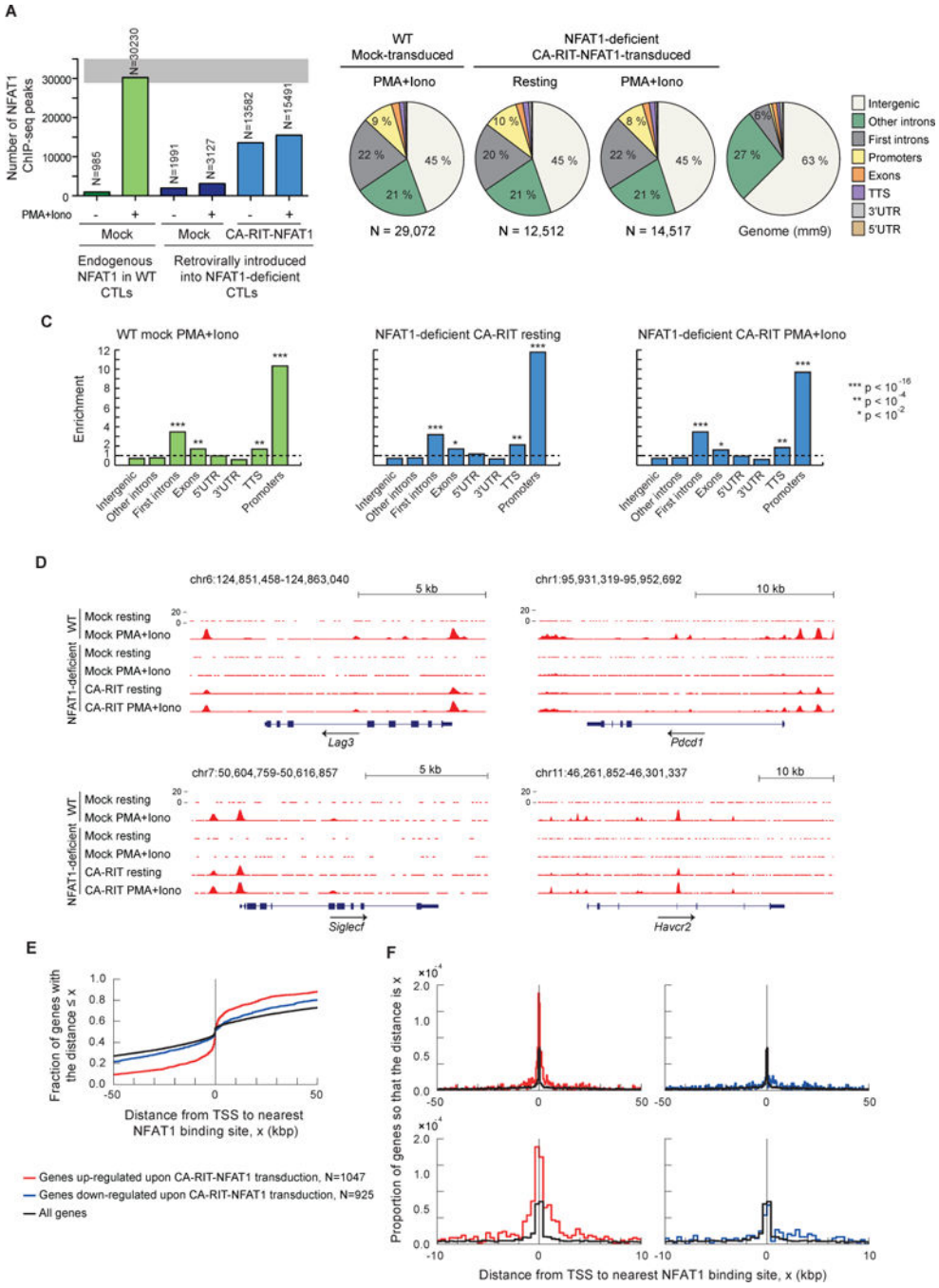

Figure 3. CA-RIT-NFAT1 directly upregulates gene expression by binding to promoter regions

ChIP-seq results for endogenous NFAT1 in WT cells and for CA-RIT-NFAT1 in transduced NFAT1-deficient cells, either untreated or restimulated with PMA and ionomycin for 1h. (**A**) Number of NFAT1 and CA-RIT-NFAT1 ChIP-seq peaks identified by HOMER. (**B**) Pie charts show the genomic distribution of ChIP-seq peaks for endogenous NFAT1 in WT cells transduced with empty vector (*left pie chart*), or CA-RIT-NFAT1 ChIP-seq peaks in NFAT1-deficient cells transduced with CA-RIT-NFAT1 (*middle two pie charts*). Representation of the annotated regions in the mouse mm9 genome is shown for comparison

(*right pie chart*). (**C**) Enrichment of NFAT1 binding sites in annotated genomic regions based on their relative abundance in the mouse genome (mm9). Statistical analysis was performed using Fisher's exact test. ***, p<2e-16; ** p<1e-10; * p<1e-2. (**D**) Genome browser views of *Lag3*, *Pdcd1* (encoding PD-1), *Siglec5* and *Havcr2* (encoding Tim3) loci showing the distribution of NFAT1 and CA-RIT-NFAT1 ChIP-seq peaks. (**E–F**) Cumulative plots (**E**) or probability per base pair (**F**) of the distance between the closest NFAT1 binding site relative to the transcription start site of all genes (*black curves*), genes significantly ($p < 0.05$) upregulated (*red curves*) or downregulated (*blue curves*) in NFAT1-deficient cells transduced with CA-RIT-NFAT1 in resting conditions. See also Figure S4.

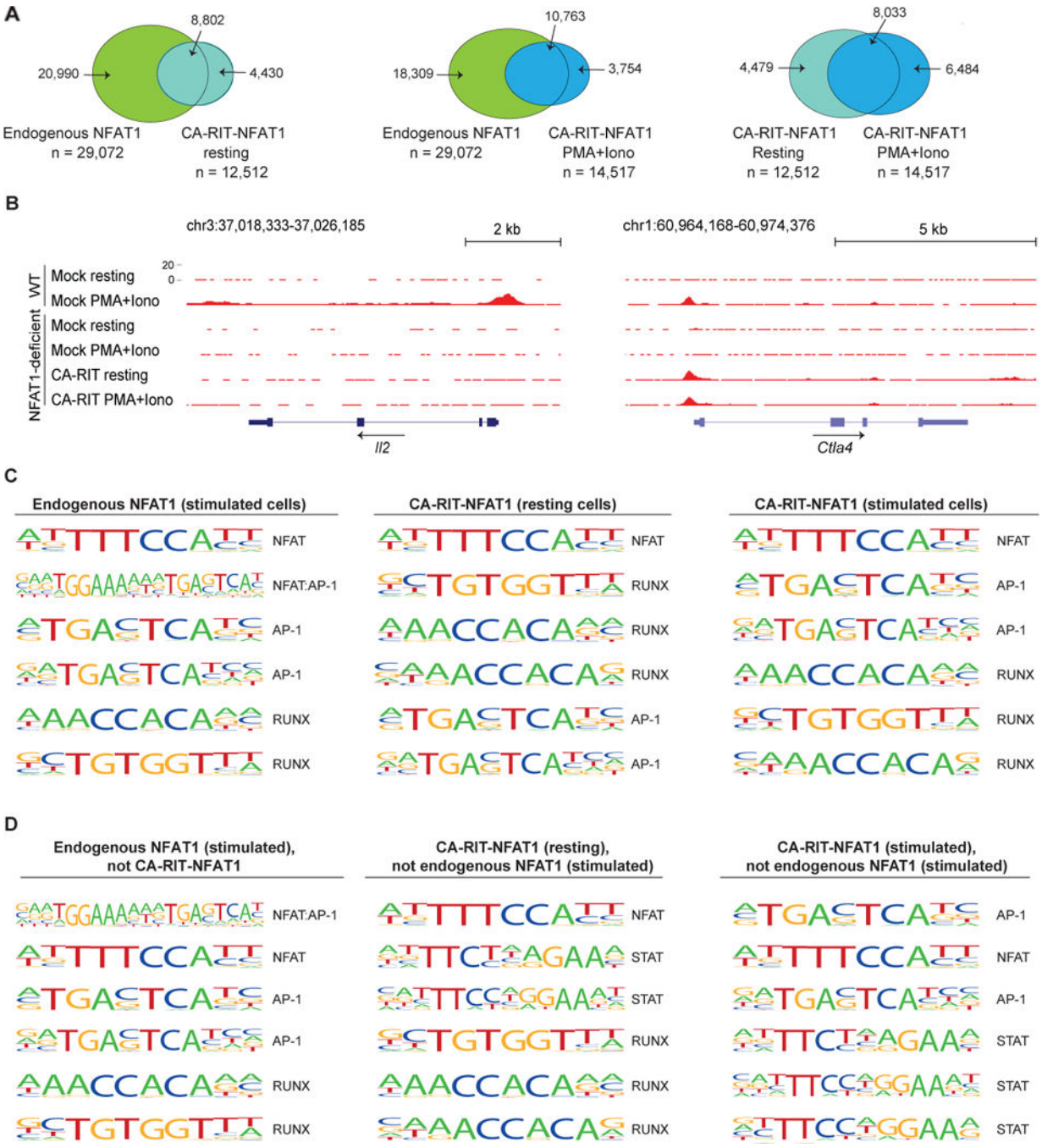

Figure 4. ChIP-seq peaks for endogenous NFAT1 are enriched for composite NFAT:AP-1 sites

(**A**) Venn diagrams showing the overlap of ChIP-seq peaks in the different conditions. (**B**) Genome browser views of *Il2* and *Ctla4* loci showing the distribution of ChIP-seq peaks. (**C**) List of the top six most representative motifs ranked based on the p-values. The HOMER program searches for published motifs, and therefore duplicate AP-1 and Runx sequences are listed. (**D**) Motifs identified as enriched only in peaks from one set of ChIP-seq data as indicated. See also Table S3.

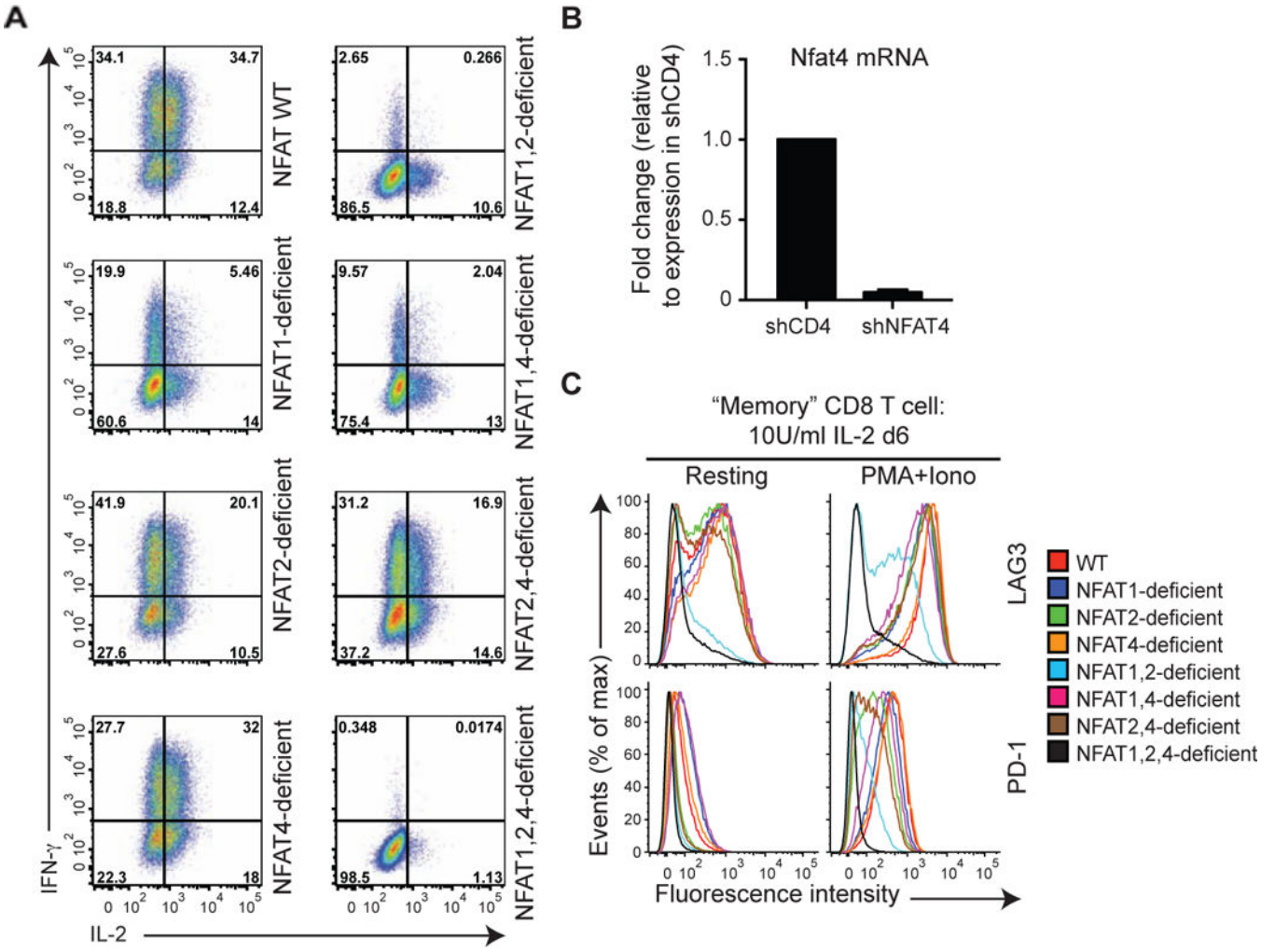

Figure 5. NFAT family members regulate the expression of inhibitory receptors *in vitro*

Naïve WT, NFAT 1-deficient, NFAT2-deficient or NFAT1, 2-deficient CD8^{+} T cells were purified by FACS, and transduced with a retrovirus encoding Ametrine (a variant GFP) and shRNAs targeting either CD4 (negative control) or NFAT4 to yield single, double or triple NFAT-deficient cells. On day 6 after activation, cells were restimulated with PMA and ionomycin for 6 h (**A and C** *right panels)*, or left untreated (**B and C** *left panels)*. IFN-y and IL-2 production (**A**) or expression of cell surface receptors (**C**) was determined by flow cytometry of Ametrine^{hi} cells. A representative experiment out of two is shown. (**B**) Expression of mRNA encoding NFAT4 was assessed by quantitative real time PCR and normalized to mRNA encoding L32 ribosomal protein. The amount of expression in control shCD4 cells was set at 1. Combined results from 3 independent experiments are shown (mean ± SEM). See also Figure S5.

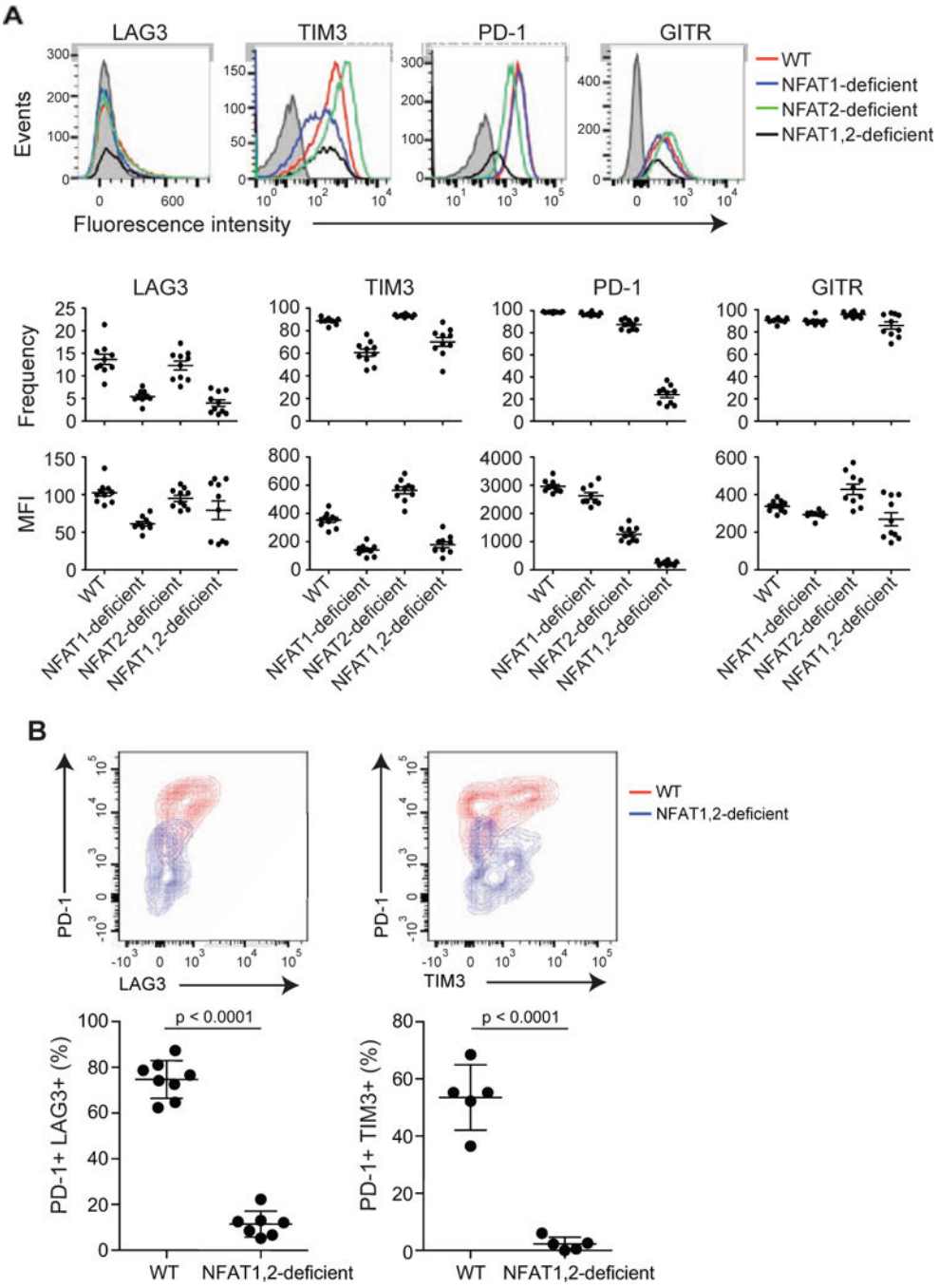

Figure 6. NFAT family members regulate the expression of inhibitory receptors *in vivo*

(**A**) Acute infection. Naïve P14^{+} *Tcra*$^{-/-}$ WT, NFAT1-deficient, NFAT2-deficient or NFAT1, 2-deficient CD8^{+} T cells (CD45.2^{+}) were transferred intravenously into CD45.1^{+} congenic mice, after which the mice were injected with LCMV (2×10^{5} PFU) intraperitoneally. Eight days after infection, splenocytes were harvested and the expression of inhibitory receptors on the adoptively transferred CD8^{+} CD45.2^{+} cells was evaluated. *Top panel*, a representative example for each genotype is shown; *bottom panels*, data for 8–10 mice in each group are summarized as mean ± SEM, with each dot representing a mouse. A

representative experiment out of two is shown. The gray histogram shows unstained control. (**B**) Chronic infection. WT mice and mice lacking both NFAT1 and NFAT2 in T cells were infected with LCMV clone 13. Eighteen days after infection, splenocytes were harvested and expression of inhibitory receptors on $CD8^+$ $CD44^+$ H2Db-gp33-41^+ cells was determined by flow cytometry. *Top panel*, representative contour plots. *Bottom panel*, results from individual mice (2–3 independent experiments; each mouse is represented by a dot). p values were calculated using t-test.

Table 1

Partial list of genes expressed in exhausted and/or anergic T cells that are also induced in CA-RIT-NFAT1-expressing CD4 and CD8 T cells

The table shows representative genes (identified by RNA-seq) that are significantly induced in $CD4^+$ and $CD8^+$ T cells upon CA-RIT-NFAT1 expression and also overlap with genes expressed in *in vivo*-generated anergic and exhausted T cells.

Cell surface receptors and ligands		
Lag3	Lymphocyte-activation gene 3	*
Tnfrsf9	Tumor necrosis factor receptor superfamily member 9; 4-1BB	*
Ptger2	Prostaglandin E2 receptor 2	*
Havcr2	Hepatitis A virus cellular receptor 2; TIM-3	*
Alcam	Activated Leukocyte cell adhesion molecule	*
Tigit	T cell immunoreceptor with Ig and ITIM domains	+
Ctla4	Cytotoxic T-Lymphocyte Antigen 4	+
Ptger4	Prostaglandin E2 receptor 4	+
Tnfrsf1b	Tumor necrosis factor receptor superfamily member 1b	+
Ccl4	Chemokine (C-C motif) ligand 4	+
CD109	Cluster of Differentiation 109	#
CD200	Cluster of Differentiation 200; Ox-2	#
Tnfsf9	Tumor necrosis factor superfamily member 9; 4-1BBL	#
Nrp1	Neuropilin-1	#
Sema4c	Semaphorin-4C	#
Ptprj	Receptor-type tyrosine-protein phosphatase eta	#
Il21	Interleukin 21	#
Tspan2	Tetraspanin-2	#
Transcription factors		
Ikzf2	IKAROS family zinc finger 2; Helios	*
Egr2	Early growth response protein 2	*
Tox	Thymocyte selection-associated high mobility group box protein	*
Zeb2	Zinc finger E-box-binding homeobox 2	*
Irf4	Interferon Regulatory Factor	*
Nfatc1	Nuclear Factor of Activated T cells c1; NFAT2	*
Zbtb32	Zinc finger and BTB domain-containing protein 32; ROG	#
Rbpj	Recombinant binding protein suppressor of hairless	#
Hif1a	Hipoxia-inducible factor 1-alpha	#
Signaling		
Rgs16	Regulator of G-protein signaling 16	*
Sh2d2a	SH2 domain-containing protein 2A	+
Nucb1	Nucleobindin-1	+
Plscr1	Phospholipid scramblase 1	+
Ptpn11	Tyrosine-protein phosphatase non-receptor type 11	#
Prkca	Protein kinase C alpha (PKCa)	#

Plscr4	Phospholipid scramblase 4	#
Others		
Casp3	Caspase 3	*
Gpd2	Glycerol-3-phosphate dehydrogenase	+
Gas2	Growth arrest-specific protein 2	+
Sh3rf1	SH3 domain containing ring finger 1	#
Nhedc2	Na+/H+ exchanger domain containing 2	#
Plek	Pleckstrin	#
Tnfaip2	Tumor necrosis factor, alpha-induced protein 2	#
Ctsb	Cathepsin B	#

* genes that are upregulated in both anergic and exhausted T cells;

+ genes whose expression is significantly upregulated in exhausted T cells but is not statistically significant in anergic T cells;

genes whose expression is significantly upregulated in anergic T cells but is not statistically significant in exhausted T cells. *In vivo* data obtained from (Doering et al., 2012; Okamura et al., 2009; Wherry et al., 2007).